AIP Journal of Applied Physics

Analysis of ringing effects due to magnetic core materials in pulsed nuclear magnetic resonance circuits

N. Prabhu Gaunkar, N. R. Y. Bouda, I. C. Nlebedim, R. L. Hadimani, I. Bulu, K. Ganesan, Y. Q. Song, M. Mina, and D. C. Jiles

Citation: Journal of Applied Physics **117**, 17E508 (2015); doi: 10.1063/1.4916753
View online: http://dx.doi.org/10.1063/1.4916753
View Table of Contents: http://scitation.aip.org/content/aip/journal/jap/117/17?ver=pdfcov
Published by the AIP Publishing

JOURNAL OF APPLIED PHYSICS **117**, 17E508 (2015)

Analysis of ringing effects due to magnetic core materials in pulsed nuclear magnetic resonance circuits

N. Prabhu Gaunkar,[1,a)] N. R. Y. Bouda,[1] I. C. Nlebedim,[1] R. L. Hadimani,[1] I. Bulu,[2] K. Ganesan,[2] Y. Q. Song,[2] M. Mina,[1] and D. C. Jiles[1]
[1]*Department of Electrical and Computer Engineering, Iowa State University, Ames, Iowa 50011, USA*
[2]*Schlumberger-Doll Research, Cambridge, Massachusetts 02139, USA*

(Presented 6 November 2014; received 29 September 2014; accepted 23 November 2014; published online 3 April 2015)

This work presents investigations and detailed analysis of ringing in a non-resonant pulsed nuclear magnetic resonance (NMR) circuit. Ringing is a commonly observed phenomenon in high power switching circuits. The oscillations described as ringing impede measurements in pulsed NMR systems. It is therefore desirable that those oscillations decay fast. It is often assumed that one of the causes behind ringing is the role of the magnetic core used in the antenna (acting as an inductive load). We will demonstrate that an LRC subcircuit is also set-up due to the inductive load and needs to be considered due to its parasitic effects. It is observed that the parasitics associated with the inductive load become important at certain frequencies. The output response can be related to the response of an under-damped circuit and to the magnetic core material. This research work demonstrates and discusses ways of controlling ringing by considering interrelationships between different contributing factors. © *2015 AIP Publishing LLC*. [http://dx.doi.org/10.1063/1.4916753]

I. INTRODUCTION

The phenomenon of nuclear magnetic resonance (NMR) is widely used to study different materials through NMR spectroscopy. This technique can also be used for *in-situ* investigation of earth formations.[1] NMR measurements are thus an important part of oilfield well-logging and are used to identify and quantify oil and gas reservoirs. For these measurements, an "inside-out" approach is employed.[2] NMR well-logging uses the NMR response of an earth formation to determine its porosity and permeability. A continuous record is obtained along the length of a borehole in an operation. The NMR equipment comprises large static magnetic fields, generally produced by permanent magnets, and a high frequency oscillatory magnetic field projecting outwards from the core of the test apparatus. The two magnetic fields interact with the surrounding media and the received signal is then studied to determine the porosity and hydraulic permeability of the media. Unlike conventional NMR systems, inside-out NMR measurements are conducted at resonant frequencies below 2 MHz.[3] The weak nature of the static magnetic fields employed[2] makes it difficult to observe the chemical shifts and hence most of the signal information is obtained from the relaxation data or the free induction decay (FID) signal. Oil-well NMR tools are used to conduct NMR measurements within the ground and the received signals can be analyzed *in-situ* or once the tool is brought to the surface. Thus, these tools require the lowest FID time to maximize the number of measurements and attain a high signal to noise ratio (SNR). However, the antenna imposes a limitation to these measurements. The antenna forms an LRC subcircuit and undergoes signal damping at certain resonant frequencies. The damped signal can superimpose over the NMR echo signals and may mask the actual NMR signal.[4] Several methods[5–9] like using a Q switch, transformer-coupled matching networks, snubber circuits, etc., have been employed to reduce the effect of this signal damping. However, complete elimination of the damping has not been achieved. Another parameter that can be varied to control the signal damping is the core material used within the antenna. A magnetic core is used within the antenna to enhance the contribution of the alternating or radio-frequency (RF) magnetic field in the zone of interest. Its main function is to enhance the inductance of the RF sensor and increase the signal-to-noise ratio. Thus, core materials with higher magnetic permeability are preferred. Generally, soft magnetic core materials are utilized for down-hole NMR applications. These core materials also contribute to the signal damping or ringing. In this paper, we investigate the decay profiles of different magnetic core materials used for NMR applications. A relation between the signal ringing, circuit parameters, and magnetic properties of the materials is established.

II. THEORY

A. Pulsed NMR

All NMR measurement techniques are based on the interaction of the nuclear spins and an externally applied magnetic field. The nuclear spin precesses about the axis of the external magnetic field. The precession frequency (Larmor frequency) can be mathematically described as

$$\omega = \gamma B, \tag{1}$$

where γ, the proportionality constant, is called the gyromagnetic ratio, B corresponds to the static magnetic field, and ω

[a)]Author to whom correspondence should be addressed. Electronic mail: neelampg@iastate.edu.

corresponds to the Larmor frequency. A perpendicular RF field is applied in the form of short bursts. The application of this pulse creates a state wherein the phases of the different spins are partially correlated. Thus, the RF pulse is applied to create a state of spin coherence. In the presence of both the RF field and the external magnetic field, the net magnetic spin moment rotates about the axis of the resulting effective field. Since the external static field is much larger than the RF field, the precession frequency with respect to the static field would be very high. To eliminate the dominance of the static field, the RF field rotates at a frequency equal to the precession frequency. The spins then rotate about the axis of the perpendicular RF field until the RF field is turned off.

B. Ringing effects and FID

RF pulses are repeatedly applied to the test sample and the signal received during this time is know as the FID. It is found that the magnetization does not precess indefinitely and the spins return back to their original state after removal of the RF pulse. This phenomenon is known as relaxation. Two time constants, T_1 and T_2, are used to describe this behavior. T_1 corresponds to the gain and loss of magnetization along the direction of external magnetic field. T_2 or the damping time constant corresponds to loss of phase coherence among the nuclei or the loss of magnetization along the direction of the orthogonal RF field. Mathematically, T_2 is related to the linewidth ($\Delta\nu_{1/2}$) of the signal through the relation

$$\Delta\nu_{1/2} = \frac{1}{\pi T_2}. \tag{2}$$

Loss of magnetization energy in the direction of the static field or along the RF field would be equivalent, i.e., reduction of T_1(or T_2) would lead to faster signal magnetization and faster signal acquisition.[10] In this study, the FID signal is characterized as ringing since the test specimen is considered to be the magnetic core within the coil. This ringing effect caused due to the magnetic core may lead to erroneous measurements due to emergence of false resonant peaks. The ringing in pulsed NMR systems can be attributed to several sources such as acoustic ringing,[11] eddy current damping effects,[12] magnetostriction effects,[11] material related effects, and circuit and sensing system designs.[10] Isolating the contributions of the different causes is necessary to understand and systematically decrease or eliminate the detrimental effects of ringing.

C. LRC subcircuit

The antenna introduces parasitic capacitances and resistances in the overall circuit. At higher frequencies, these circuit elements, especially the capacitance, affects the overall system operation. The circuit behaves like an underdamped LRC circuit. The FID signal that is observed can then be correlated to the behavior of an underdamped LRC circuit. Mathematically, it can be described as

$$V(t) = e^{-(\alpha t)}[A_1 \cos(\omega_o t) + A_2 \sin(\omega_o t)]. \tag{3}$$

Here, ω_o corresponds to the resonant frequency, A_1 and A_2 correspond to the amplitude, and α corresponds to the decay constant. The FID signal is damped due to the presence of the series resistance.

III. EXPERIMENTAL DETAILS

Measurements are conducted using commercially available magnetic core materials. Different materials with relative permeabilities: Mu55, Mu100, Mu125, and Mu1200 were selected. The NMR measurement set-up comprises several units: a NMR spectrometer, high-power rf amplifier, signal duplexer, and an inductive antenna. A system level diagram can be found in Fig. 1. The user enters several parameters through a menu-driven program and activates the NMR spectrometer. The spectrometer generates the RF pulse with a maximum output power level of 1 mW. The amplitude and phase of this signal are controlled by the inbuilt digital signal processor. The generated signal is then sent to the high-power RF amplifier and is amplified up to a maximum power level of 4000 W and passed on to the duplexer. The duplexer serves a dual function. It allows the high-power signal to reach the antenna and blocks it from reaching the spectrometer thus preserving it from any damage. A timing signal ensures coherence between the signals from the spectrometer, amplifier, and duplexer. The RF pulse is then applied to the antenna. Initially, a short pulse of duration 20 μs is selected in order to obtain a larger frequency bandwidth. Once the resonance peaks are identified, selective pulses of approximately 200 μs are applied. This allows the user to focus at a particular frequency. The pulses from the receiver are acquired with a delay of 400 μs to allow the amplifier signal to switch off. The received signal is once again re-routed to the NMR spectrometer via the duplexer and a pre-amplifier. The free inductive decay signal can then be analyzed. The system-level timing is illustrated in Fig. 2. A permanent magnet with a field strength of 400 G is used to generate the static magnetic field.

Since the NMR signal is very weak, measurements are repeated every 500 ms in order to improve the signal to noise ratio, and the signal is then averaged. The amplitude and position of the signal are repeated. The stochastic nature of noise makes it unrepeatable at the same location after each iteration.

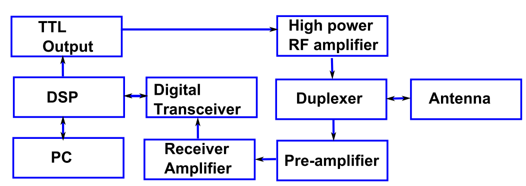

FIG. 1. System-level block diagram.

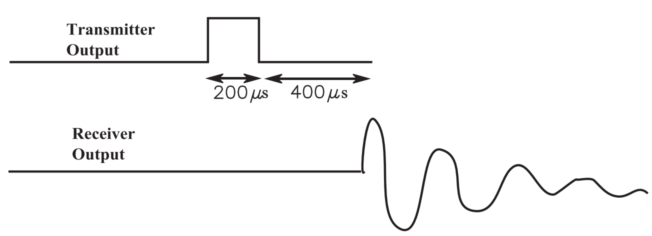

FIG. 2. System timing diagram. A sinusoidal pulse train is transmitted for a duration of 200 μs and the signal at the receiver is recorded 400 μs after the pulse is turned off. The received signal is described as the FID.

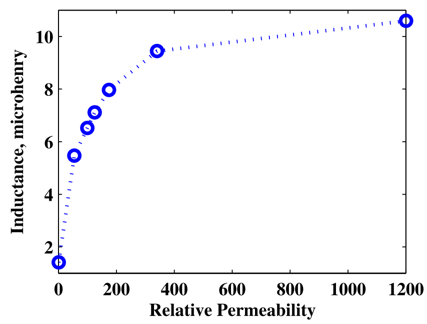

FIG. 3. Inductance vs relative permeability. Inductance was measured using an LRC meter in the 10 kHz frequency range. Relative permeability was estimated from the manufacturer's specifications.

IV. RESULTS AND DISCUSSION

Since a non-resonant antenna is employed, the inductive core material dominates the signal response. As seen in Fig. 3, with an increase in the material permeability, the inductance increases. It was found that higher permeability materials also resulted in higher ringing and multiple resonant frequencies.

A. Quantification of ringing

The damped nature of the signal allows us to propose a figure of merit (FOM) that could be utilized to quantify the ringing. As illustrated in Fig. 4, the FOM can be mathematically defined as

$$FOM = \frac{V_1 - V_2}{V_0(t_1 - t_2)}, \quad (4)$$

where V_1 is the original signal amplitude at time t_1 once the RF pulse is suspended, V_2 is the amplitude of the FID after time t_2, and V_0 is equivalent to the initial ringing amplitude. The difference between t_1 and t_2 was selected to be equal to 1 time constant though a decay by 5 time constants would be a better approximation, since it would account for complete signal decay. For this study, the proposed FOM may be used to compare the ringing in different magnetic materials.

B. Effect of material on signal decay time

The input pulse frequency is swept over a frequency range of 0.1 to 1.4 MHz and the corresponding resonant frequencies are recorded for each ferromagnetic material. The FID for each of these frequencies was estimated. In order to observe the effect of material on the signal damping, the FID signals are compared at a frequency (f_o) of 152 kHz for all materials except Mu1200 which indicated resonance at a frequency of 140.5 kHz. This frequency may be considered an indication of the circuit resonance. A comparison of the signal decay time can be found in Fig. 5. The ringing signals were fitted using varied exponential functions. The decay time was computed in each case and the line width was approximated from the Fourier spectrum of the signal. The results are summarized in Table I.

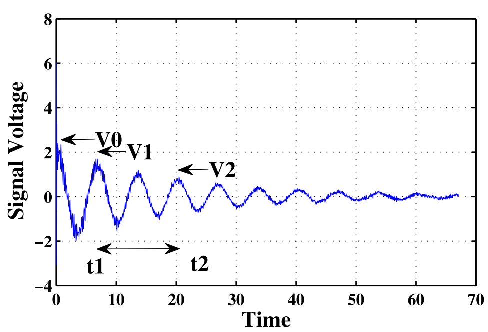

FIG. 4. Figure of merit. V_1 was considered to be the same as V_0. Δt which equals t_1–t_2 was considered to be one time constant.

For a typical FID signal, the initial signal amplitude may relate to the permeability of the material as seen in Fig. 5. This signal will completely mask the NMR signal due to the high ringing amplitude. Thus, high permeability materials or impregnated materials may not be good candidates for the magnetic core in the inductive antenna. This leads to a trade-off since it is necessary to use a high permeability core material in the NMR tool to allow maximum flux penetration in the surrounding earth.

For a typical FID signal, the signal decay time also provides information about the texture and the type of fluid in

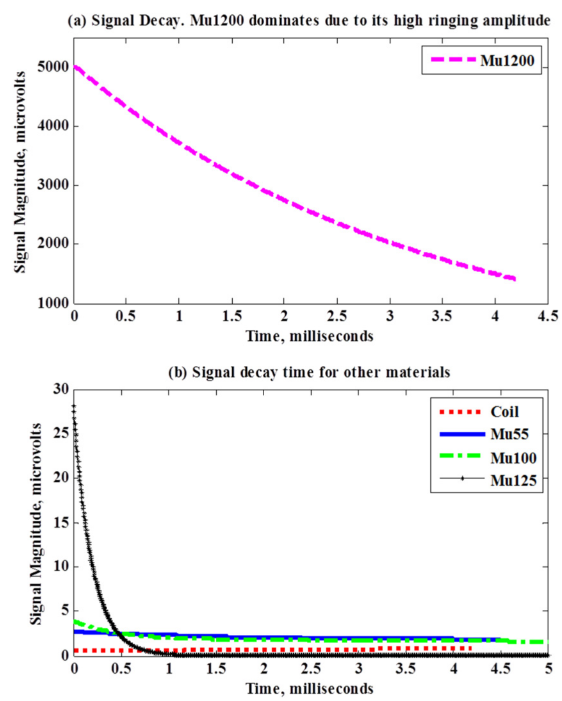

FIG. 5. Signal decay profiles. Decay times were estimated from the exponential fits. The decay time was approximated when the signal had decayed by one time constant or was 0.37 of its original value.

TABLE I. Comparison of signal decay profiles at single frequency.

Material	Initial ringing amplitude ($\|\mu V\|$)	Approx. decay time (ms)	Approx. line width (Hz)
Coil only	0.57	…	346.19
Mu55	2.518	9.034	307.3
Mu100	3.95	16.9	277.6
Mu125	27.03	0.2	403
Mu1200	5048	3.278	293

an NMR application. It is observed that with a decrease in the porosity of the core material, as in the case of Mu125 (impregnated material), the ringing amplitude decreased and there was a significant reduction in the signal decay time.

C. Effect of material on Q-factor

With an increase in inductance, the quality (Q) factor directly increases. A Q factor above 0.5 corresponds to an underdamped circuit oscillation. The single-sided frequency spectrum of the time-domain signals is observed in Fig. 6. The frequency spectrum is shifted such that the center frequency at the origin corresponds to the resonant frequency of 152 kHz and 140.5 kHz for Mu1200. The center frequency for Mu1200 is offset by approximately 0.2 kHz. Materials with a greater line width indicate correspondingly wider peaks in the frequency spectrum and lower Q factors. From Table I, it is found that Mu125 has the highest line width and correspondingly lowest decay time. The FOM is found to decrease with an increase in signal decay time as observed in Table II.

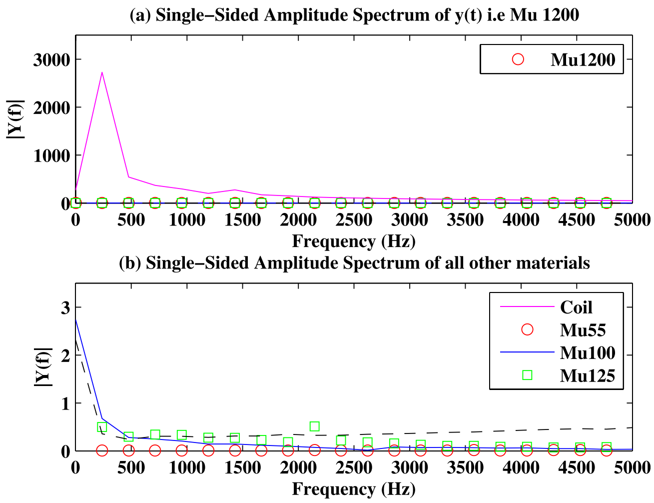

FIG. 6. Shifted frequency spectrum. The frequency at the origin corresponds to the resonant frequency of each material.

TABLE II. Comparison of magnetic materials at single frequency.

Material	Inductance (μH)	Quality factor	FOM (Hz)10^{-3}
Coil only	1.41	13.85	…
Mu55	5.47	45.84	0.0697
Mu100	6.525	50.71	0.0372
Mu125	6.798	52.36	3.15
Mu1200	10.59	52.28	2.1141

The magnetostrictive effects were also investigated for the soft magnetic materials. It was found that around 400 G field, the materials under test had already saturated and there was no change in the strain of the sample. Thus, at the operating dc magnetic field strengths of NMR, the materials will not show any changes in strain.

V. CONCLUSIONS

This study indicated that certain soft magnetic materials greatly affect the free inductive decay observed in NMR systems. This leads to an increase in signal decay time and in turn significant dead time in the receiver. Among the materials tested, it was found that despite their high permeability, Mu125 and Mu1200 had significantly smaller decay times compared to Mu55 or Mu100. Mu125 displayed the least signal decay time. However, the signal due to the magnetic core material may mask the actual NMR signal due to its high initial ringing amplitude. The observations made in this study indicate that further work on design and selection of appropriate magnetic core materials, probably incorporating properties of tailor made functional nano-composites, may allow us to develop a mechanism for controlling the ringing effects in NMR systems.

ACKNOWLEDGMENTS

This research was funded by Department of Electrical and Computer Engineering, Iowa State University and Schlumberger-Doll Research.

[1]R. L. Kleinberg and J. A. Jackson, Concepts Magn. Reson. **13**, 340 (2001).
[2]R. L. Kleinberg, A. Sezginer, D. Griffin, and M. Fukuhara, J. Magn. Reson. (1969) **97**, 466 (1992).
[3]D. Griffin, R. Kleinberg, and M. Fukuhara, Meas. Sci. Technol. **4**, 968 (1993).
[4]F. Bert, V. Simonet, B. Canals, J. Robert, S. Petit, and H. Mutka, École thématique de la Société Française de la Neutronique **13**, 03001 (2014).
[5]S. Zhang, X. Wu, and M. Mehring, Chem. Phys. Lett. **173**, 481 (1990).
[6]H. Dong, Y. Zhang, H.-J. Krause, X. Xie, A. I. Braginski, and A. Offenhäusser, Supercond. Sci. Technol. **22**, 125022 (2009).
[7]L. B. Casabianca, D. Mohr, S. Mandal, Y.-Q. Song, and L. Frydman, J. Magn. Reson. **242**, 197 (2014).
[8]S. Mandal, S. Utsuzawa, D. Cory, M. Hürlimann, M. Poitzsch, and Y.-Q. Song, J. Magn. Reson. **242**, 113 (2014).
[9]S. Utsuzawa, S. Mandal, and Y.-Q. Song, J. Magn. Reson. **216**, 128 (2012).
[10]T. Hopper, S. Mandal, D. Cory, M. Hürlimann, and Y.-Q. Song, J. Magn. Reson. **210**, 69 (2011).
[11]G. Mamniashvili, Y. Sharimanov, T. Gegechkori, A. Akhalkatsi, T. Gavasheli, and D. Gventsadze, in Proceedings of DIPED (2012).
[12]M. S. H. Akram, Y. Terada, I. Keiichiro, and K. Kose, J. Magn. Reson. **245**, 1 (2014).